

K and evolutionary corrections from UV to IR

B.M. Poggianti

¹ Dipartimento di Astronomia, vicolo dell'Osservatorio 5, 35122 Padova, Italy

² Kapteyn Instituut*, P.O. Box 800, 9700 AV Groningen, The Netherlands, bianca@astro.rug.nl

Received; accepted

Abstract. ¹

K and evolutionary corrections are given for the E, Sa and Sc Hubble types for the *U, B, V, R, I, J, H, K* filters of the Johnson – Bessell & Brett photometric system and the *gri* filters of the modified Thuan & Gunn system up to the redshift $z = 3$. Their dependence on the time scale of star formation in ellipticals is investigated.

The corrections are computed according to an evolutionary synthesis model that reproduces the integrated galaxy spectrum in the range 1000-25 000 Å; such a model makes use of an infrared observed stellar library and its results are compared with nearby galaxies.

Evolving spectral energy distributions of the various Hubble types, as well as optical-IR and IR-IR colour evolution and adopted filter response functions are also given.

Key words: galaxies: evolution – galaxies: photometry – galaxies: distances and redshifts – galaxies: fundamental parameters – cosmology: miscellaneous

1. Introduction

The *K* corrections for galaxies of different morphological types are necessary to interpret the magnitude-redshift relation, the luminosity function of galaxies and for most of the spectrophotometric studies of distant objects.

The *K* correction is defined as the corrective term that needs to be applied to the observed magnitude in a certain band due to the effect of redshift. It does not take into account the effects of galactic evolution; when this cannot be neglected, it is necessary to apply a further correction, the evolutionary one (EC), that can be computed by using spectrophotometric models. Considering the fact that present observations reach high redshifts and progressively fainter magnitudes, establishing the connection

between distant and local galaxies requires more and more often the knowledge of the galactic evolution and the use of both the corrections.

A number of authors have previously published tables of *K* corrections (Hubble 1936; Humason et al. 1956; Oke & Sandage 1968; Schild & Oke 1971; Whitford 1971; Oke 1971; Wells 1972; Pence 1976; Ellis et al. 1977; Code & Welch 1979; Coleman et al. 1980; Frei & Gunn 1994). In most of the cases these works are limited for one of more of the following aspects: the number of photometric bands, the number of galactic types, the maximum redshift considered. Many of the papers mentioned above only deal with ellipticals, that are considered the best standard candles at high redshifts. The biggest efforts to supply an extended set of *K* corrections have been made from Pence (1976) and Coleman et al. (1980). Pence computed the *K* corrections for the *U, B, V, R* filters of the Johnson system and the *R* Sandage's filter for the following morphological types; E/S0, Sab, Sbc, Scd, Im with a maximum redshift of 2.18. Coleman et al. (1980) found *K* corrections in the *U, B, V, R* bands for the bulges of M31 and M81 and for Sbc, Scd, Im with a $z_{max} = 2$. Frei & Gunn (1994) have used the energy distribution of Coleman et al. to compute the *K* corrections at $z = 0.1, 0.2, 0.4, 0.6$ of E, Sbc, Scd and Im for five photometric systems (Johnson *UBV*, Gullixson et al. *B_jRI*, Thuan and Gunn *gri*, *u'g'i'r'z'* and Cousins *RI*).

These studies make use of an empirical method: with a software programme, the observed spectral energy distribution of a given morphological type (averaged over a number of objects) is redshifted. The *K* corrections are then computed from these mean curves and using the filter transmission functions; in this case there is no need to assume a given cosmological model. With this method it is obviously not possible to compute the evolutionary corrections, for which the most direct computing method is making use of a model of spectrophotometric evolution.

Another advantage of using models instead of observations is that, in order to cover a wide range of redshift, the latter often requires the connection of observations in various spectral regions, most of the times obtained with dif-

* Present address

¹ Tables 3-41 are only available in electronic form at the CDS via anonymous ftp to cdsarc.u-strasbg.fr (130.79.128.5) or via <http://cdsweb.u-strasbg.fr/Abstract.html>.

ferent instrumentation; such a connection requires a great accuracy, introduces an uncertainty and moreover the necessary observations are not always available. On the basis of models, Bruzual (1983) calculated the *total* corrections ($K+EC$) and the total magnitudes (including K , EC and luminosity distance) for the Johnson's B, V, K bands and the Koo-Kron F band. Bruzual's model did not include the most advanced stellar evolutionary phases, that dominate the integrated flux in the ultraviolet (Post-AGB) and the infrared (AGB) region. From their spectrophotometric model, Guiderdoni & Rocca-Volmerange (1988) computed the predicted apparent magnitudes and colours of distant galaxies for the Johnson U, B, V, R, I filters, Koo-Kron U^+, J^+, F, N, gr from Thuan & Gunn and some broad-band filters from the Faint Object Camera and the Wide Field Camera of the Hubble Space Telescope, taking into account also the nebular emission and the internal extinction. Buzzoni (1995) presented total corrections ($K+EC$) computed from an evolutionary synthesis model for an elliptical in the Johnson's B, V, K bands and Gunn gr_i until a redshift of 1 for different cosmological parameters.

In this paper both the K and the evolutionary corrections are given for a set of photometric bands including infrared ones (J, H, K). They are computed from an evolutionary synthesis model and an attempt has been made to cover a wide range of morphological types for sufficiently small intervals of redshift up to $z = 3$.

2. Definitions and adopted cosmological parameters

In this paragraph the K and EC formulae will be presented in detail, in order to facilitate the use of the following tables. The definitions that follow are taken from Tinsley (1970).

Consider a galaxy at a redshift z , observed at the present epoch t_0 , whose light was emitted at the time t_1 . Let's define $E(\lambda, t)$ as the monochromatic luminosity measured at the wavelength λ at the time t in its rest frame, in units $\text{ergs sec}^{-1}\text{\AA}^{-1}$ or equivalent.

L_{λ_0} is defined as the observed luminosity in the band with effective wavelength λ_0 (in $\text{ergs s}^{-1}\text{cm}^{-2}$):

$$L_{\lambda_0} = \int_0^\infty l_\lambda S(\lambda) d\lambda \quad (1)$$

where $S(\lambda)$ is the transmission function of the instrument and l_λ is the observed monochromatic flux ($\text{ergs s}^{-1}\text{\AA}^{-1}\text{cm}^{-2}$) at the wavelength λ . Then the following equation is valid:

$$\begin{aligned} L_{\lambda_0} &= \frac{1}{4\pi D^2(1+z)} \int_0^\infty E\left(\frac{\lambda}{1+z}, t_1\right) S(\lambda) d\lambda \\ &= \frac{\int_0^\infty E(\lambda, t_0) S(\lambda) d\lambda}{4\pi D^2(1+z)} \cdot \frac{\int_0^\infty E\left(\frac{\lambda}{(1+z)}, t_0\right) S(\lambda) d\lambda}{\int_0^\infty E(\lambda, t_0) S(\lambda) d\lambda} \end{aligned}$$

$$\frac{\int_0^\infty E\left(\frac{\lambda}{1+z}, t_1\right) S(\lambda) d\lambda}{\int_0^\infty E\left(\frac{\lambda}{1+z}, t_0\right) S(\lambda) d\lambda} \quad (2)$$

being D the luminosity distance. Equation (2) can be written as:

$$\begin{aligned} m_{\lambda_0} &= M(\lambda_0, t_0) + 5 \log D + \text{constant} \\ &+ \left[2.5 \log(1+z) + 2.5 \log \frac{\int_0^\infty E(\lambda, t_0) S(\lambda) d\lambda}{\int_0^\infty E\left(\frac{\lambda}{1+z}, t_0\right) S(\lambda) d\lambda} \right] \\ &+ 2.5 \log \frac{\int_0^\infty E\left(\frac{\lambda}{1+z}, t_0\right) S(\lambda) d\lambda}{\int_0^\infty E\left(\frac{\lambda}{1+z}, t_1\right) S(\lambda) d\lambda} \end{aligned} \quad (3)$$

The term in the square brackets is the K correction and the last term is the evolutionary correction. From Eq.(3) the observed magnitude m_{λ_0} for the band with effective wavelength λ_0 is equal to the sum of five terms:

- a) the absolute magnitude in the same band as it would be measured in the rest frame at the epoch of observation t_0 . This is indicated as $M(\lambda_0, t_0)$ and corresponds to the numerator of the first term in the Eq.(2);
- b) a term that only depends on the luminosity distance D ;
- c) a constant term, depending only on the band used, that determines the normalization of the absolute magnitude;
- d) the K correction;
- e) the evolutionary EC correction.

The K correction is the difference between the observed magnitude of the galaxy of age t_0 measured at the wavelength $\lambda_1 = \lambda_0/(1+z)$ and the magnitude of the same galaxy of age t_0 computed at λ_0 . Notice that t_0 is the moment of observation (~ 15 Gyr), while t_1 is the time at which the light has been emitted. Therefore the K correction corresponds to the difference in magnitude of two objects with identical spectrum due to the redshift: it does not include in any way the intrinsic evolution of the spectrum due to the evolution of the stellar populations that contribute to it.

On the contrary, the EC correction depends on the intrinsic evolution of the spectral energy distribution (SED), being the difference between the magnitude of a galaxy of age t_1 and the same galaxy evolved (whose spectrum is different from the one of the previous galaxy) of age t_0 , both computed at λ_1 . It is therefore the difference in absolute magnitude measured in the rest frame of the galaxy at the wavelength of emission.

The sum of the K and EC corrections is the difference between the magnitude of a galaxy of age t_1 redshifted and the one of the evolved galaxy observed at the time t_0 at $z=0$. Both corrections are computed on the basis of models of spectrophotometric evolution, assuming a star formation history for each morphological type and having

fixed the cosmological parameters. In the general case $q_0 \neq 0.5$ it is valid

$$t = \frac{-4q_0}{H_0(1-2q_0)^{3/2}} \times \left[\frac{\sqrt{\frac{1+2q_0z}{1-2q_0}}}{2 \left[1 - \left(\frac{1+2q_0z}{1-2q_0} \right) \right]} + \frac{1}{4} \log_e \left| \frac{1 + \sqrt{\frac{1+2q_0z}{1-2q_0}}}{1 - \sqrt{\frac{1+2q_0z}{1-2q_0}}} \right| \right] \quad (4)$$

where t is the look-back time, H_0 is the Hubble constant, q_0 is the deceleration parameter and z is the redshift. The tables have been computed for $q_0 = 0.225$ and $H_0 = 50 \text{ Kms}^{-1} \text{ Mpc}^{-1}$, corresponding to an age of the Universe $t_0 = 15 \text{ Gyr}$. Corrections for different cosmological parameters can be computed directly from the evolving SEDs presented in Tables 6-29. If one prefers to define the corrections with respect to the *observed* SED of a given galaxy, the adopted model present-day SEDs given in Tables 3-5 can be replaced with the observed SED.

3. The spectrophotometric model

This work makes use of an evolutionary synthesis model that reproduces the integrated spectrum of a galaxy. A description of this model is also given in Poggianti & Barbaro (1996); here the essential informations are presented.

The emission of the stellar component is computed with a modified version of the model by Barbaro & Olivi (1986, 1989 (BGOF)), that synthesizes the SED of a galaxy in the spectral range 1000-10000 Å. The BGOF model includes, besides the main sequence and the central helium burning phase, also the advanced stellar evolutionary phases such as AGB and Post-AGB. It takes into account the chemical evolution of the galaxy, therefore the contribution to the integrated spectrum of stellar populations of different metallicities. This model has been successfully employed in the studies of star clusters in the Magellanic Clouds and of elliptical galaxies (Barbaro & Olivi 1986, 1989, 1991; Barbaro 1992; Barbaro et al. 1992).

The stellar evolutionary background has not been changed, while updates have been made to the library of stellar spectra: the new Kurucz stellar atmosphere models (version 1993) have replaced the previous ones (Kurucz 1979) and the computation of the spectrum has been extended up to 25000 Å. In the infrared region, for stars with $T_{eff} > 5500 \text{ K}$ Kurucz's models (1992) have been used. For stars with lower effective temperatures the library of observed stellar spectra by Lançon-Rocca Volmerange (1992, LRV) has been employed: such spectra cover the spectral range 14500-25000 Å, with a resolution between 25 and 70 Å. The connection between the optical spectra (1000-10000 Å) and the LRV spectra has been made by means of black body curves. For each star the black body temperature has been determined by imposing that the

resulting colours reproduce the observed ones (Koornneef 1983 ($V-K$, $J-K$, $H-K$); Bessell & Brett 1988 ($V-I$, $V-K$, $J-H$, $H-K$, $J-K$)).

A set of models of the different types has been computed for an age 15 Gyr and for all the evolutionary times corresponding to various redshifts according to Eq.(4). The SFR of an elliptical is approximated with an exponentially decreasing function and the average metallicity is assumed solar. Two time scales have been explored as e-folding times of the SFR: 1 Gyr (E) and 1.4 (E2). For the spirals, Auddino (1992) galaxy model have been employed: this is a chemical evolutionary model that includes an inflow and assumes the SFR to be proportional to the gas fraction. This model provides the SFR and the metallicity as a function of time for galaxies in the type range Sa-Sd. The model parameters for each Hubble type are determined requiring the model SED to reproduce the observed colours of local galaxies. The SEDs obtained from this model reproduce the spectral emission and absorption characteristics of local galaxies (Barbaro & Poggianti 1996), as well as their observed average gas fractions.

The inclusion of very advanced stellar phases of extremely metal rich stars (Greggio & Renzini 1990) could modify the evolutionary corrections of ellipticals for the bluest bands at redshifts ≥ 0.5 , because the evolution of the ultraviolet spectral region would be influenced by this kind of stellar objects. The K corrections would not be affected, being the SED of local ellipticals well reproduced by the models also in the UV range. Anyway the metallicity of stars in ellipticals is still uncertain: the Mg_2 index, commonly used to estimate the global metallic content, is difficult to interpret, due to the excess in early-type galaxies of the ratio between the α elements (among which oxygen and magnesium) and the iron with respect to the solar value.

Concerning the spirals, the models do not take into account the intrinsic extinction due to the presence of dust, that is expected to be progressively more significant at increasing redshifts and at decreasing effective wavelength. In some cases it will be necessary to consider a further correction for intrinsic extinction (Di Bartolomeo et al. 1995).

3.1. Comparison with nearby galaxies

In principle a first test of the model could be done by comparing the results with the observations of integrated SEDs of star clusters; good candidates are the young star clusters in the Magellanic Clouds (Barbaro & Olivi 1991). However a great dispersion in the infrared colours of these objects has been observed; such a dispersion is explained considering the stochastic fluctuations in the mass distribution of the evolved stars (Barbaro 1992). For this reason and for the uncertainty in the determination of the age and the metallicity of each cluster, the comparison has

Table 1. Colours of the models of age 15 Gyr

	$(U - B)$	$(B - V)$	$(V - R)$	$(R - I)$	$(V - J)$	$(V - H)$	$(V - K)$	$(J - H)$	$(J - K)$	$(H - K)$
El1	0.53	0.95	0.76	0.67	2.25	2.95	3.23	0.71	0.98	0.28
El2	0.45	0.91	0.71	0.60	2.02	2.65	2.90	0.63	0.87	0.25
El3	0.37	0.86	0.67	0.54	1.86	2.42	2.65	0.57	0.79	0.22
Sa	0.33	0.85	0.69	0.60	2.01	2.65	2.90	0.64	0.89	0.25
Sb	0.21	0.77	0.66	0.58	1.95	2.57	2.82	0.63	0.87	0.24
Sc	0.02	0.63	0.59	0.54	1.80	2.40	2.63	0.60	0.83	0.23
Sd	-0.09	0.52	0.53	0.48	1.62	2.18	2.40	0.56	0.78	0.22

been made with galaxies, for which the stochastic effects are expected negligible.

Table 1 presents the colours of models of age 15 Gyr of different morphological types; in the case of the elliptical, the dependence of colours from the average metallicity is shown: solar (El1, correspondent to the E model), $Z=0.01$ (El2) and $Z=0.005$ (El3). Notice that the optical-IR colours ($(V - J)$, $(V - H)$, $(V - K)$) change drastically with the Hubble type, while the IR-IR colours ($(J - H)$, $(J - K)$, $(H - K)$) change slightly along the type sequence, with differences comparable to the observative uncertainty.

Observations in the near-IR have been obtained from Persson et al. (1979) for early-type galaxies in Virgo, in Coma and in the field and from Bower et al. (1992a,b) for a sample of early-type objects in Virgo and in Coma. The average galaxy colours observed by the different authors, corrected for redshift, reddening and aperture effects, are compared in Table 2 with the model results for ellipticals of various metallicities. The agreement is satisfactory. Persson et al. corrected the colours by using Schild & Oke (1971) and Whitford (1971) V -band K -corrections; for the infrared bands, they computed the corrections using several late-type stars from Woolf et al. (1964). Bower et al. defined the U and V band K corrections from a series of template early-type galaxy SEDs, among which those of Coleman et al., and the infrared K -corrections from the SED of the K3 giant star α Tau (Woolf et al. 1964). For spirals, a great dispersion in the infrared colours *within* the same morphological type is observed (Gavazzi & Trinchieri 1989), therefore spirals are not included in Table 2; the colours of the models for the spirals are inside the range of observed values.

Moreover the updated evolutionary synthesis model has been used successfully in the studies of galaxies at intermediate redshifts (Poggianti & Barbaro 1995, 1996).

4. Presentation of the tables and the figures

From the spectral energy distributions and from the response functions of the filters in the various bands, the K and EC corrections have been computed; they are presented in Tables 31-38. The corrections have been com-

puted up to $z = 3$ for the bands U, B, V, R, I, J, H, K of the Johnson's photometric system (B_1 and B_2 corresponding to B_2 and B_3 from Buser (1978) and J, H, K from Bessel & Brett 1988) and gri of the Thuan & Gunn system (1976) as modified from Schneider et al. (1983). The B magnitude is computed considering the sum of the two filter response functions B_1 and B_2 divided by two. Being 1000 Å the lower limit of the wavelengths considered from the model, the U and B bands have been computed respectively up to $z = 2$ and $z = 2.5$.

The response function of the filters are given in Tables 39-41; it is useful to underline that, due to a typing error in Table 4 from Bessell & Brett, the definition of the H and K bands can be ambiguous. It is indispensable, in any case, to check the response function of any filter of interest; in the case of the K band, the difference between the filter here adopted and that in *the figure* of Bessell & Brett can give rise to errors in the corrections of 0.2 maximum.

The spectral energy distributions of the models of different Hubble types of age 15 Gyr are given in the Tables 3-5 for the E, Sa and Sc in the spectral range 1012-27 000 Å. The SEDs are also presented in Fig. 1. From top to bottom (at 1000 Å) the spectra of the Sc, Sa, E2 and E are shown; it is visible that the difference between the spectra of the two ellipticals is significant only at the shortest wavelengths. The rest frame spectra of evolving SEDs of different ages are presented in Fig. 2 (E), Fig. 3 (Sa) and Fig. 4 (Sc); the ages shown are 15, 13.2, 10.6, 8.7, 7.4, 5.9, 4.3, 3.4 and 2.2 Gyr, corresponding respectively to the redshifts: 0, 0.1, 0.3, 0.5, 0.7, 1.0, 1.5, 2.0, 2.5, 3.0. Such SEDs are given in Tables 6-29, from which the interested user can compute any desired property.

Considering the high metal content adopted and the observed correlation between the Mg_2 index and the absolute luminosity, the elliptical model is representative of luminous objects. Due to the observed substantial variations of the ultraviolet flux with the galactic luminosity, the results presented here cannot be applied to low luminosity ellipticals (i.e. with a lower metal content) for redshifts ≥ 0.5 . Furthermore, the differences between the two model ellipticals ($\tau = 1$ and $\tau = 1.4$ Gyr) appear sig-

Table 2. Comparison models-observations for early-type galaxies; *=ellipticals only, without S0

		$(U - V)$	$(V - K)$	$(J - K)$	$(J - H)$	$(H - K)$
Bower et al.:	Virgo	1.39	3.17	0.86	–	–
	Coma	1.40	3.13	0.88	–	–
Persson et al.:	Campo	–	3.29	0.86	0.66	0.20
	Virgo	–	3.22	0.86	0.65	0.21
	Coma	–	3.19*	–	–	–
E11		1.48	3.23	0.98	0.71	0.28
E12		1.36	2.90	0.87	0.63	0.25
E13		1.23	2.65	0.79	0.57	0.22

nificant starting from $z = 0.6$ (K correction) and $z = 0.20$ (EC correction) in the bluest bands.

In order to obtain the observed colour of the progenitor galaxy of a given type of local galaxy the following relation can be used:

observed colour=colour of the local corresponding galaxy + (difference between the K corrections of the first and the second band)+ (difference between the EC corrections of the first and the second band).

This relation can be deduced from Eq.(3). For instance, if one wants to compute the expected observed colour ($V - J$) of an elliptical at $z = 1$:

$$\text{colour of a local elliptical } (V - J) = 2.25$$

$$K_V = 3.42, K_J = 0.28$$

$$K_V - K_J = 3.14$$

$$EC_V = -1.87, EC_J = -0.96$$

$$EC_V - EC_J = -0.91$$

$$\text{expected observed colour} = 2.25 + 3.14 - 0.91 = 4.48.$$

Figures 5-15 show the K and EC corrections for different bands; the sudden change in all the curves at $z = 2.5$ is due to the fact that the last two models have been computed with a large redshift step (0.5). Considering the smooth behaviour of these functions between a redshift 2.5 and 3, a smaller redshift step is not required.

Figures 16-23 show the rest frame and observer's frame colour evolution.

In Table 30 model K_V corrections are compared with those of Pence for negligible Galactic extinction. The differences, starting at relatively low redshift for the latest types, are partly due to the slightly dissimilar response functions adopted and mainly to the differences in the SEDs. It must be stressed that two galaxies classified of the same type on the basis of their morphological appearance (spiral arms, bulge to disk ratio etc.) can have significantly different spectra, indicative of unlike present and past star formation rates. Therefore the model galactic sequence should be interpreted as a "star formation" sequence, while the results found with an empirical method will necessarily depend on the single galaxies chosen for the sample. For this reason the comparison of the two methods results rather difficult. Furthermore Pence him-

self defined the ultraviolet observations available to him (preliminary OAO data) as "somewhat uncertain", especially for E/S0. Moreover, due to the lack of ultraviolet observations for the Sbc, Pence had to interpolate between the types Sab and Scd. Coleman et al.'s results for bulges are in agreement with elliptical results from Pence until a redshift $\simeq 0.75$ in the V band. They found instead substantial differences from Pence in the K_U of the elliptical for $z > 0.3$, probably due to the UV Pence's difficulties mentioned above. A better agreement is obtained between their results and the model values presented here.

5. Summary

K and evolutionary corrections from UV to IR are presented for three kinds of galactic types (E, Sa and Sc) for a number of filters in two photometric systems. Corrections in other photometric systems are available by request (Koo-Kron U^+, J^+, F, N (Koo 1985), Cousin R, I (Bessell 1986), B_J, R_F of Couch & Newell (1980) and 418, 502, 578, 685, 862 of the Durham group (Couch et al. 1983)).

These results are based on an evolutionary synthesis model that successfully reproduces the colours and the shape of the continuum of the various galactic types of local and distant galaxies.

Spectral energy distributions of the different Hubble types are given in a wide spectral range (1012-27000 Å) and allow one to compute K corrections for any other photometric system.

Acknowledgements.

I wish to express my thanks to G. Barbaro, for suggestions and corrections that improved the text, and to A. Cohen, for helping in typing the tables and enjoying life.

References

- Auddino M., 1992, Master Degree Thesis, University of Padova
- Barbaro G., 1992, Mem. Soc. Astron. Ital. 63, 127
- Barbaro G., Olivi F.M., 1986, Spectrophotometric Models of Galaxies. In: Chiosi C., Renzini A. (eds.) Spectral Evolution of Galaxies. Reidel, Dordrecht, p. 283
- Barbaro G., Olivi F.M., 1989, ApJ 337, 125 (BOGF)

- Barbaro G., Olivi F.M., 1991, AJ 101, 922
 Barbaro G., Poggianti B.M., 1996, A&A submitted
 Barbaro G., Bertola F., Burstein D., 1992, Mem. Soc. Astron. Ital. 63, 505
 Bessell M.S., 1986, PASP 98, 1303
 Bessell M.S., Brett J.M., 1988, PASP 100, 1134
 Bower R.G., Lucey J.R., Ellis R.S., 1992a, MNRAS 254, 589
 Bower R.G., Lucey J.R., Ellis R.S., 1992b, MNRAS 254, 601
 Bruzual A.G., 1983, Rev. Mex. Astron. Astrofis. 8, 63
 Buser R., 1978, A&A 62, 411
 Buzzoni A., 1995, ApJS in press
 Code A.D., Welch G.A., 1979, ApJ 228, 95
 Coleman G.D., Chi-Chao Wu, Weedman D.W., 1980, ApJS 43, 393
 Couch W.J., Newell E.B., 1980, PASP 92, 746
 Couch W.J., Ellis R.S., Godwin J., Carter D., 1983, MNRAS 205, 1287
 Di Bartolomeo A., Barbaro G., Perinotto M., 1995, MNRAS 227, 1279
 Ellis R.S., Fong R., Phillips S., 1977, Nat 265, 313
 Frei Z., Gunn J.E., 1994, AJ 108, 1476
 Gavazzi G., Trinchieri G., 1989, ApJ 342, 718
 Greggio, L., Renzini A., 1990, ApJ 364, 35
 Guiderdoni B., Rocca-Volmerange B., 1988, A&AS 74, 185
 Hubble E.P., 1936, ApJ 84, 517
 Humason M.L., Mayall N., Sandage A.R., 1956, AJ 61, 97
 Koo D.C., 1985, AJ 90, 418
 Koornneef J., 1983, A&A 128, 84
 Kurucz, R., 1979, ApJS 40, 1
 Kurucz R., 1992, Model Atmospheres for Population Synthesis. In: Barbu B., Renzini A. (eds.) The Stellar Populations of Galaxies, IAU Symp. n.149. Kluwer, Dordrecht, p.225
 Kurucz R. 1993, CD-Rom n.13, version 22/10/93
 Lançon A., Rocca-Volmerange B., 1992, A&AS 96, 593 (LRV)
 Oke J.B., 1971, ApJ 170, 193
 Oke J.B., Sandage A.R., 1968, ApJ 154, 21
 Pence W., 1976, ApJ 203, 39
 Persson S.E., Frogel J.A., Aaronson M., 1979, ApJS 39, 61
 Poggianti B.M., Barbaro G., 1995, Mem. Soc. Astron. Ital. vol.65, n.3, p.953
 Poggianti B.M., Barbaro G., 1996, A&A in press
 Schild R.E., Oke J.B., 1971, ApJ 169, 209
 Schneider D.P., Gunn J.E., Hoessel J.G., 1983, ApJ 264, 337
 Thuan T.X., Gunn J.E., 1976, PASP 88, 543
 Tinsley B.M., 1970, Ap&SS 6, 344
 Wells D.C., 1972, PhD Thesis, University of Texas
 Whitford A.E., 1971, ApJ 169, 215
 Wolf N.J., Schwarzschild M., Rose W.K., 1964, ApJ 140, 833

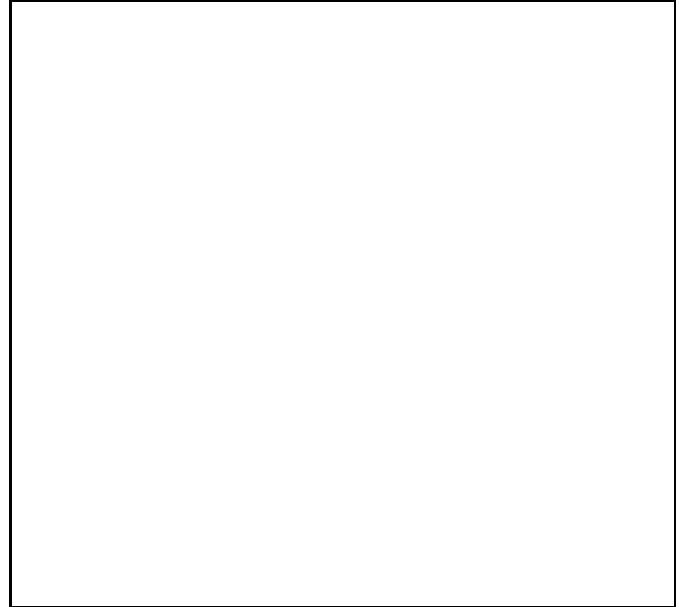


Fig. 1. SEDs of 15 Gyr old models normalized at 5500 Å. From top to bottom (at 1000 Å): Sc (dotted line); Sa (short dashed line); E2 (long dashed line); E (solid line)



Fig. 2. SEDs of the elliptical model for 9 redshifts: 0, 0.1, 0.3, 0.5, 0.7, 1.0, 1.5, 2.0, 2.5, 3.0



Fig. 3. SEDs of the Sa model for the same redshifts of Fig. 2



Fig. 4. SEDs of the Sc model for the same redshifts of Fig. 2

Fig. 5-15. K and EC corrections: the solid line represents the elliptical with e-folding time 1 Gyr; the dotted line the elliptical with $\tau = 1.5$ Gyr (E2); the short dashed line refers to the Sa and the long dashed line to the Sc. In some cases the curves of the two ellipticals are superimposed and therefore indistinguishable

Fig. 16-23. Rest frame and observer's frame colour evolution: the former case is denoted by the "0" subscript. Symbols as in Figs. 2-12